Indian Journal of Chemistry
Vol. 53A, April-May 2014 pp. 499-503

Mineralization of aqueous organic pollutants using a catalytic plasma reactor

P Manoj Kumar Reddy, Sk Mahammadunnisa & Ch Subrahmanyam*

Energy and Environmental Research Laboratory, Department of Chemistry,
Indian Institute of Technology Hyderabad, Hyderabad 502 205, Andhra Pradesh, India
Email: csubbu@iith.ac.in

Received 6 December 2013, revised and accepted 18 February 2014

Electrical discharges generated at water-gas interface in a dielectric barrier discharge reactor has been utilized for the degradation and mineralization of a model aqueous organic pollutant, viz., methyl orange. Mineralization of the dye is identified by an online infrared gas analyzer and confirmed by a total organic carbon analyzer. It has been observed that both degradation efficiency and mineralization of the dye increases on addition of modified alumina catalyst to the plasma reactor. On addition of FeO_x/Al_2O_3 catalyst, the mineralization efficiency increases from 31% with plasma reactor alone to 38%. It has been observed that dye degradation followes first-order kinetics and degree of mineralization increases as a function of time with decreasing energy yield.

Keywords: Catalyst, Dye degradation, Degradation, Dielectric barrier discharge reactor, Catalytic plasma reactor, Plasma reactor, Energy yield, Mineralization, Nonthermal plasma, Total organic carbon, Methyl orange, Iron oxide, Alumina

Aqueous organic pollutants pose a serious environmental problem and their increasing concentrations have been a major concern[1-5]. For treatment of these pollutants, conventional treatments may not be effective, especially for mineralizing the pollutant[6]. Dyes are toxic organic compounds and may lead to formation of some non-degradable intermediates that may have potential carcinogenicity and mutagenicity[7,8]. To address this issue, various chemical and physical treatments have been proposed. The essential idea behind these techniques is to remove the dyes either by adsorption and/or catalytic oxidation[9-18]. However, many of these tested methods are not effective in mineralizing the dye and in the best practiced method i.e., adsorption, the pollutant is transferred to another phase, hence it cannot offer a permanent solution[19]. On the other hand, biological processes such as anaerobic/aerobic degradation, may have limited applicability due to long reaction durations.

Alternative methods based on advanced oxidation processes (AOPs) for wastewater treatment have been proposed. Among the AOPs, nonthermal plasma (NTP) generated by electrical discharges is a promising technique[20-22]. Methyl orange (MO) is an important example of azo dye and has been widely used in textiles, foodstuffs, paper and leather industries. The treatment of wastes containing methyl orange has also been widely reported[12,16,22,24]. Various plasma reactors have been developed for the wastewater treatment. NTP operated in dielectric barrier discharge (DBD) configuration is of particular interest, mainly due to the presence of energetic electrons that may excite, dissociate and ionize water molecules to form active species, which drive the degradation and mineralization processes[25]. For the effective utilization of these short lived species, metal oxide catalysts like Al_2O_3, Fe_2O_3, SiO_2, TiO_2 and ZnO are often integrated with NTP. These catalysts facilitate the ***in situ*** decomposition of ozone, leading to the formation of atomic oxygen which is a stronger oxidant than ozone[26,27]. Among these, aluminum oxides (Al_2O_3) catalysts are attractive due to their high surface area and can be loaded with a variety of metal oxides. Also, as operation of plasma reactors in aqueous media is known to produce hydrogen peroxide a combination of iron oxide catalysts is more logical to facilitate Fenton type reaction.

Our previous work demonstrated the importance of the ozone decomposition, hydroxyl radicals and hydrogen peroxide formation and their utility during the degradation of organic compounds, including crystal violet, methylene blue and endosulfan[7,25,28-30]. The present study focuses on application of catalytic NTP-DBD reactor for the degradation and mineralization of a common textile dye, viz., methyl

orange. For this purpose, Al_2O_3, Fe/Al_2O_3 catalysts are prepared by combustion synthesis and characterized by X-ray diffraction and nitrogen adsorption. The influence of different parameters such as applied voltage, initial concentration and addition of the catalyst has been investigated.

Materials and Methods

Preparation and characterization of catalyst

Methyl orange, $Al(NO_3)_3.6H_2O$ and $Fe(NO_3)_3.9H_2O$ were received from Merck, India. Al_2O_3, 10wt% $FeOx/Al_2O_3$ was prepared by combustion synthesis method. In a typical synthesis[31], metal precursor was added to citric acid to maintain the fuel to oxidant ratio at 1. The desired amount of aqueous solution of nitrate salt and citric acid was sonicated for 15 minutes and simultaneously stirred to obtain a homogenous mixture and then transferred into a quartz crucible. Then the mixture was placed in a preheated furnace maintained at 673 K for 5 min. The stoichiometric equation of aluminium nitrate and citric acid is as follows:

$$2Al(NO_3)_3 + 1.67C_6H_8O_7 \rightarrow Al_2O_3 + 10CO_2 + 6.68H_2O + 3N_2 \quad \ldots (1)$$

$$2Al(NO_3)_3 + Fe(NO_3)_3 + 2.34C_6H_8O_7 \rightarrow FeOx/Al_2O_3 + 14CO_2 + 9.3H_2O + 4.5N_2 \quad \ldots (2)$$

The isotherms surface area of the samples was determined by nitrogen adsorption-desorption by using Quantachrome Instruments model Nova 2200. Typically, 0.1g of catalyst was used for each analysis. Prior to the analysis the samples were degassed at 300 °C for 2 h. XRD analysis was performed by using Cu Kα (λ = 1. 54 A°) radiation on a X'Pert Pro, PAN analytical diffractometer. Sample preparation for XRD analysis involved placing the finely ground catalyst on a sample holder. The X-ray tube was operated at 40 kV and 30 mA.

Plasma reactor

The design of the plasma reactor and the details are given elsewhere[25]. Briefly, the electrical discharge was created in a parallel plane coaxial NTP-DBD reactor with the operating voltage varied between 14 and 20 kV (Jayanthi Transformers) at 50 Hz frequency. The applied voltage was measured with a 1000:1 high voltage probe (Agilent 3413g6A). The reactor is a coaxial quartz cylinder with an inner diameter of 19 mm and wall thickness of 1.6 mm. Silver paste painted on the outer surface of the quartz tube acts as the outer electrode, whereas a cylindrical stainless steel rod serves as the inner electrode[25]. The discharge length was 20 cm and discharge gap was fixed at 3.5 mm. Gas flow rate was regulated by a mass flow controller (Alborg) and was fed into the plasma reactor with a Teflon tube. The energy yield of the degradation was calculated[24, 25] from Eq. (3),

$$\boldsymbol{Y}(\text{g/kWh}) = \frac{C(\text{g/l}) \times V(\text{L}) \times \frac{1}{100} \times \text{Conv}(\%)}{P(\text{kW}) \times t\ (\text{h})} \quad \ldots (3)$$

where $\boldsymbol{C}$ is the initial dye concentration, $\boldsymbol{V}$ is the volume of the solution, $\boldsymbol{P}$ is power and $\boldsymbol{t}$ is time. It has been observed that increasing applied voltage increases the power and decreases the energy yield.

The high voltage was applied to the inner electrode, while the outer electrode was grounded. The total charge, $\boldsymbol{Q}$, was recorded by measuring the voltage across a capacitor connected series to the ground electrode. The voltage and charge waveforms were monitored by a four channel digital storage oscilloscope with 100 MHz and 1G/s (Tektronix Oscilloscope TDS 2014B), and the voltage and charge (V-Q) waveforms were recorded by an oscilloscope. The charge and voltage waveforms were plotted to get the Lissajous figure. The power dissipated in the discharge can be calculated by multiplying Lissajous figure area with the operating frequency[23].

Dye degradation

The concentration of the dye was measured as a function of time on UV-visible spectrophotometer (T90UV/VIS spectrometer, PG Instruments, UK) at a wavelength of 464 nm. The degradation percentage was calculated by Eq. (4),

$$\text{Degrad. (\%)} = \frac{C_0 - C_t}{C_0} \times 100 \quad \ldots (4)$$

where $\boldsymbol{C}_o$ and $\boldsymbol{C}_t$ are the initial and the final concentrations of dye solution respectively.

The total organic carbon (TOC) was measured by using a Shimadzu TOC-V_{CPH} total organic carbon analyzer. The mineralization percentage was calculated by using Eq. (5),

$$\text{TOC removal (\%)} = \frac{t_0 - t_t}{t_0} \times 100 \quad \ldots (5)$$

where $\boldsymbol{t_0}$ and $\boldsymbol{t_t}$ are the initial and the final TOC concentrations of MO, respectively.

Ozone concentration at the outlet of the reactor was measured with an UV-absorption ozone monitor (API 450 NEMA Teledyne Instruments). It was observed that ~300 ppmv of ozone was released at the outlet in the absence of a catalyst.

Results & Discussion

Catalyst characterization

The XRD patterns of the catalyst are shown in Fig. 1; the peak corresponding to the ***d***-spacing value of 1.979Aº (400 plane) confirms the formation of γ-alumina. Characteristic peaks of iron oxide for Fe/Al_2O_3 indicates the metal oxide loading on Al_2O_3. Textural characterization was carried out by nitrogen adsorption-desorption isotherms at 77 K and surface area was calculated by using the BET equation. The specific surface area, total pore volume and average pore diameter of the samples are listed in Table 1. The surface area of Al_2O_3 was ~280 m^2/g, which decreased slightly to ~255m^2/g on loading with Fe/Al_2O_3.

Degradation studies

Electric discharge at the water-gas interface is one of the advanced oxidation processes that offers specific advantages like generation of multiple oxidants. The electrical breakdown in water produces UV radiation, shock wave, ions (H^+, H_3O^+, O^+, H^-, O^-, OH^-), molecular species (H_2, O_2, H_2O_2), and, most importantly, reactive radicals[25-30] such as $O^{\bullet}$, $H^{\bullet}$ and $OH^{\bullet}$. These active chemical species are responsible for MO degradation. MO degradation studies were carried out at varying concentrations of MO (50, 75 and 100 mg/L) as a function of the applied voltage, which was varied from 14-18 kV. The results shown in Fig. 2 indicate that, during the degradation of 50 ppm of the dye, within 30 min of plasma treatment 84% of dye was degraded at 14 kV, which increased to 91% at 18 kV. The degradation efficiency decreases with increasing concentration, as shown in Fig. 2b. For example, after 30 min of treatment, at 18 kV, 91% degradation was achieved for 50 ppm, which decreased to 80% for 100 ppm.

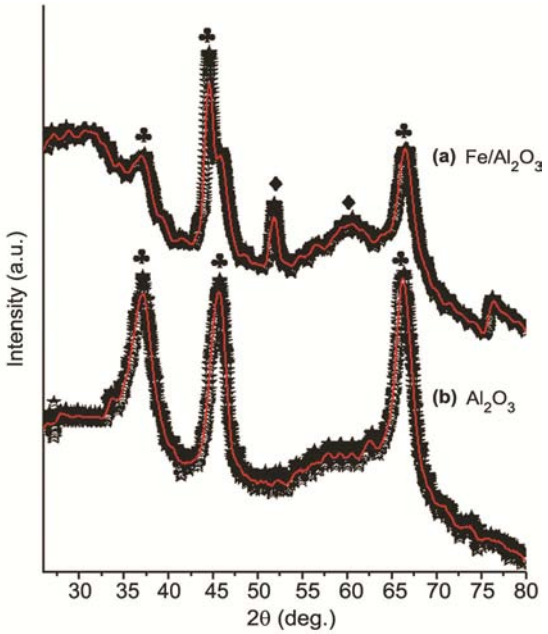

Fig. 1 – XRD patterns of the catalysts. [(a) Al_2O_3; (b) Fe/Al_2O_3].

Table 1 – Physicochemical characteristics of the catalysts Al_2O_3 and Fe/Al_2O_3

	Specific surface area (m^2/g)	Pore vol. (cm^3/g)	Pore dia. (nm)
Al_2O_3	280	0.11	10.8
Fe/Al_2O_3	255	0.08	7.8

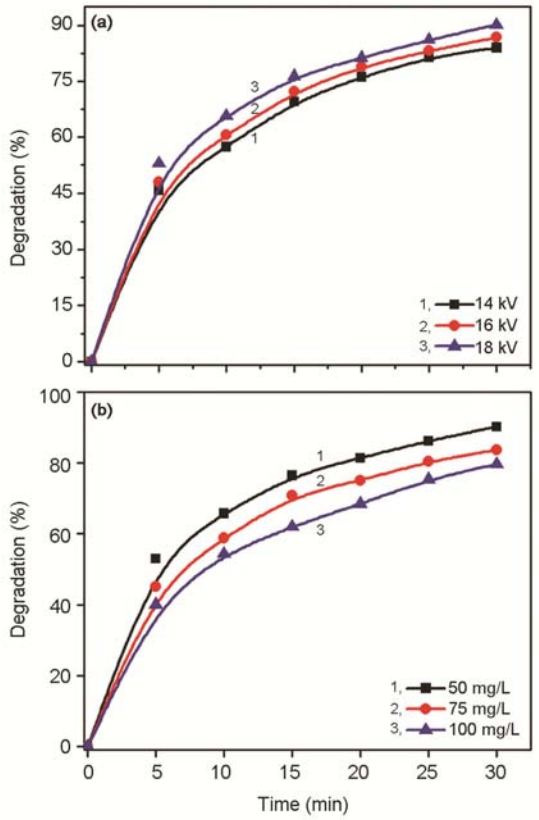

Fig. 2 – (a) Effect of applied voltage on MO degradation for 50 ppm initial concentration. [1, 14 kV; 2, 16 kV; 3, 18 kV]. (b) Effect of initial concentration on MO degradation with 18 kV applied voltage [1, 50 mg/L; 2, 75 mg/L; 3, 100 mg/L].

Kinetics of degradation

In order to model a reaction, understanding kinetics is very much important. During the present study, kinetics of dye degradation followed first order kinetics and the corresponding rate constant was calculated by the following equation[25], $\ln(\boldsymbol{C}/\boldsymbol{C}_0) = -\boldsymbol{k}_1\boldsymbol{t}$, where $\boldsymbol{C}_0$ is the initial concentration of dye, $\boldsymbol{C}$t is the concentration of dye at time $\boldsymbol{t}$, and $\boldsymbol{k}$ is the observed first order rate constant (min^{-1}). The kinetics data of MO degradation as shown Fig. 3 followed a linear relationship. The coefficient indicated the linearity and confirmed the first-order kinetics behaviour.

Effect of catalyst addition

As reported earlier, NTP is non-selective and may lead to formation of undesired by-products. One of the ways of improving NTP performance is to integrate plasma with a suitable catalyst, which is capable of utilizing the reactive species produced by plasma. These reactive species may be ozone, hydrogen peroxide, etc[27-29]. Once the presence of hydrogen peroxide is confirmed, addition of Fe-catalysts may facilitate Fenton type reactions. An advantage of using iron salts is the production of hydroxyl radicals ($OH^{\bullet}$, $\boldsymbol{E}_0$ = 2.80 V) that occurs through the self-decomposition of H_2O_2 (H_2O_2, $\boldsymbol{E}_0$ = 1.78 V). In a similar manner, a catalyst capable of ozone ***in situ*** decomposition may produce atomic oxygen which has higher oxidation potential (O_3, $\boldsymbol{E}_0$ = 2.42 V) than ozone. It is worth mentioning that at 18 kV ~80 ppm H_2O_2 and 300 ppm ozone were observed in the present reactor. Hence, the effect of $Al_2O_3$and Fe/Al_2O_3 was investigated on the degradation of MO at 18 kV applied voltage (Fig. 4). The highest conversion achieved was ~93% for Fe/Al_2O_3 addition to plasma against 79% with plasma alone. Improved conversion may be either due to H_2O_2 decomposition by Fenton reaction and/or ozone decomposition as given in Eq. (6),

$$Fe^{2+} + H_2O_2 \rightarrow OH^{\bullet} + OH^{-} + Fe^{3+} \quad \ldots (6)$$

or the catalytic decomposition of ozone (Eqs 7-11),

Ozone adsorption

$$O_3 + A \leftrightarrow O_3\text{-}A \quad \ldots (7)$$

MO adsorption

$$MO + A \leftrightarrow MO\text{-}A \quad \ldots (8)$$

Reaction of adsorbed MO with adsorbed ozone

$$O_3\text{-}A + MO\text{-}A \leftrightarrow 2P\text{-}A \quad \ldots (9)$$

Desorption of products

$$2P\text{-}A \leftrightarrow 2A + CO_2 + H_2O \quad \ldots (10)$$

where 'A' represents active centers in the catalyst, MO represents methyl orange and P represents the products. Another possibility is the direct oxidation of MO by ozone as presented in Eq. 11.

$$O_3\text{-}A + MO\text{-}A \leftrightarrow P\text{-}A \quad \ldots (11)$$

Mineralization of dye

As mentioned earlier, conventional adsorption at best may transfer the pollutant to another phase against the desired mineralization that leads to the formation of CO_2 and H_2O. In order to understand the influence of catalyst addition and concentration on the mineralization of the dye, total organic carbon (TOC) analysis was carried out. During the plasma interaction, dye molecules may be destroyed by active species, followed by oxidation of the partially fragmented species by the oxidants available in the system. The azo group (-N=N-) may be converted to amines followed by organic acids and finally to CO_2.

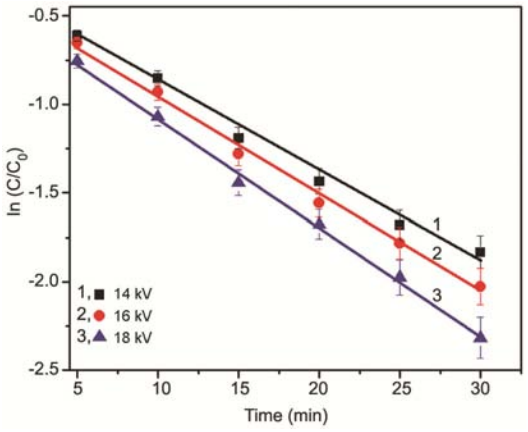

Fig. 3 – First order kinetics of MO degradation. [Appl. voltage (kV): 1, 14; 2, 16; 3, 18; initial conc. of MO: 50 ppm. [1, Al_2O_3 adsorption; 2, plasma alone; 3, Al_2O_3; 4, Fe/Al_2O_3].

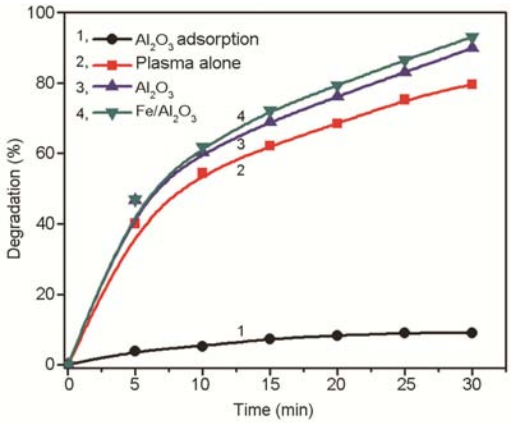

Fig. 4 – Effect of addition of catalyst on MO degradation. [Appl. voltage: 18 kV; initial conc. of MO: 100 ppm].

Qualitative analysis of CO_2 was carried out by COx analyzer[24]. At 18 kV applied voltage for 100 ppm initial concentration, plasma alone showed 31% of mineralization while with the addition of the $FeOx/Al_2O_3$ catalyst, it increased to ~38%. These results show that the, catalyst improves the mineralization as well as the performance of the reactor towards total oxidation.

Energy efficiency

The dye degradation efficiency may be better illustrated by the widely accepted energy yield, which is a measure of the amount of pollutant decomposed per unit energy[25]. In the present study, most of the dye degradation was achieved within 15 min. Detailed data of energy yield under various operating conditions is given in Table S1 (Supplementary Data). As a function of time, % degradation increases with decreasing energy yield; probably due to more energy consumption for longer durations. On increasing the applied voltage from 14 kV to 18 kV, the energy yield decreases from 23.2 g/kWh to 8.3 g/kWh for 50 mg/L. Also, with increasing the concentration from 50 mg/L to 100 mg/L, the energy yield increases from 8.3 g/kWh to 13.6 g/kWh at 18 kV applied voltage. However, in presence of the catalyst, yield increases from 13.6 to 15.8 g/kWh. This increase in the presence of the catalyst may be due to the ***in situ*** formation of oxidants like atomic oxygen, which in turn lead to hydroxyl radical formation.

Conclusions

As an alternative to conventional techniques, nonthermal plasma approach has been investigated for methyl orange degradation from aqueous solution. The advantage of NTP-DBD is the high energy efficiency and improved mineralization on addition of the catalyst. It may be concluded that NTP is effective in removing the dyes from aqueous medium. Also, the mineralization efficiency of the reactor increases on addition of the catalyst.

Acknowledgement

The authors greatly acknowledge Ministry of Environment and Forests, Govt. of India, India (Ref: No. 19-37/2008-RE), for financial support.

References

1 Chakraborty S, Basu J K, De S & Das Gupta S, ***Ind Eng Chem Res,***45 (2006) 7363.
2 Gupta V K, Mittal A, Jain R, Mathur M & Sikarwar S, ***J Colloid Interface Sci,***303 (2006) 86.
3 Bahnemann W, Muneer M & Haque M M, ***Catal Today,*** 124 (2007) 148.
4 Jones O A H, Green P G, Voulvoulis N & Lester J N, ***Environ Sci Technol,***41 (2007) 5089.
5 Anjaneyulu Y, Sreedhara Chary N & Samuel Suman Raj D, ***Rev Environ Sci Biotechnol***, 4 (2005) 273.
6 Ntengwe F W, ***Phys Chem Earth,*** 30 (2005) 734.
7 Manoj Kumar Reddy P & Subrahmanyam C, ***Ind Eng Chem Res,*** 51 (2012) 11103.
8 Ben Mansour H, Houas I, Montassar F, Ghedira K, Barillier D, Mosrati R & Chekir-Ghedira L, ***Environ Sci Pollut Res,*** 19 (2012) 2643.
9 Robinson T, Mc Mullan G, Marchant R & Nigam P, ***Biores Techno,*** 77 (2001) 255.
10 Nilamadanthai A, Sobana N, Subash B, Swaminathan B & Shanthi M, ***Indian J Chem,*** 52A (2013) 63.
11 Gupta V K, Gupta B, Rastogi A, Agarwal S & Nayak A, ***J Hazard Mater,*** 186 (2011) 901.
12 Al-Qaradawi S & Salman S R, ***J Photochem Photobiol A,*** 148 (2002) 168.
13 Brijesh P, Singh P & Jonnalagadda S B, ***Indian J Chem,*** 47A (2008) 835.
14 Manoj Kumar Reddy P, Krushnamurty K, Mahammadunnisa Sk, Mani A M & Subrahmanyam C, ***Int J Environ Sci Technol,*** (2014) (10.1007/s13762-014-0506-2).
15 Ramaraju B, Manoj Kumar Reddy P & Subrahmanyam C, ***Environ Prog Sust energy***, 33 (2014) 46.
16 Japinder K, Bansal S & Singhal Sharma S, ***Physica B***, 416 (2013) 38.
17 Lang W, Buranaboripan W, Wongchawalit J, Parakulsuksatid P, Vanichsriratana W, Sakairi N, Pathom-aree W & Sirisansaneeyakul S, ***Int J Environ Sci Technol,*** 10 (2013) 590.
18 Shanthi M & Kuzhalosai, ***Indian J Chem,*** 51A (2012) 434.
19 Manoj Kumar Reddy P, Mahammadunnisa S, Ramaraju B, Sreedhar B & Subrahmanyam C, ***Environ Sci Pollut Res***, 20 (2013) 4124.
20 Karuppiah J, Linga Reddy E, Manoj Kumar Reddy P, Ramaraju B & Subrahmanyam C, ***Int J Environ Sci Technol,*** 11 (2014) 318.
21 Karuppiah J, Linga Reddy E, Manoj Kumar Reddy, Ramaraju B, Karvembu R, & Subrahmanyam C, ***J Hazard Mater,*** 237 (2012) 289.
22 Subrahmanyam C, ***Indian J Chem,*** 48A (2009) 1068.
23 Jing C, Bangde L, Haili L & Shifu C, ***J Hazard Mater,*** 190 (2011) 706.
24 Gomathi Devi L, Girish Kumar S, Mohan Reddy K & Munikrishnappa C, ***J Hazard Mater,*** 164 (2009) 467.
25 Manoj Kumar Reddy P, Rama Raju B, Karuppiah J, Linga Reddy E & Subrahmanyam C, ***Chem Eng J***, 238 (2014) 163.
26 Muruganandham M, Chen S H & Wu J J, ***Cat Comm,*** 8 (2007) 1614.
27 Roland U, Holzer F & Kopinke F D, ***Appl Catal B,*** 58 (2005) 226.
28 Manoj Kumar Reddy P, Ramaraju B & Subrahmanyam C, ***Water Sci Technol***, 675 (2013) 1104.
29 Manoj Kumar Reddy P, Dayamani A, Mahammadunnisa S & Subrahmanyam C, ***Plasma Proc Polymers,*** 10 (2013) 1017.
30 Manoj Kumar Reddy P, Mahammadunnisa S & Subrahmanyam C, ***Chem Eng J,*** 238 (2014) 163.
31 Mahammadunnisa S, Reddy P M K, Lingaiah N & Subrahmanyam C, ***Catal Sci Technol,*** 30 (2013) 737.